

DOI: 10.13208/j.electrochem.131179

Artical ID:1006-3471(2014)05-0426-13

Cite this: *J. Electrochem.* 2014, 20(5): 426-438

Http://electrochem.xmu.edu.cn

# 杂原子掺杂碳材料氧还原催化剂研究进展

丁 炜<sup>1</sup>, 张 雪<sup>1,2</sup>, 李 莉<sup>1</sup>, 魏子栋<sup>1\*</sup>

(1. 重庆大学化学化工学院, 重庆 400044; 2. 厦门大学化学化工学院, 福建 厦门 361005)

**摘要:** 开发替代 Pt 类高活性、低成本的非贵金属燃料电池阴极氧还原催化剂是实现燃料电池商业化的必由之路。研发催化活性高, 稳定性好, 价格便宜的非贵金属催化剂是当务之急。碳纳米材料, 尤其杂原子掺杂的碳纳米材料有其独特的结构和催化性能而备受瞩目。本文结合作者课题组的研究工作, 综述了近年杂原子掺杂碳纳米材料催化剂燃料电池阴极氧电催化还原方面的研究进展。

**关键词:** 燃料电池; 氧还原; 碳掺杂; 电化学催化

**中图分类号:** O646

**文献标识码:** A

近年, 许多研究着眼于提高低温燃料电池 Pt 基催化剂的稳定性<sup>[1-2]</sup>、利用率<sup>[3]</sup>及降低电极 Pt 负载量<sup>[4-5]</sup>, 开发可完全替代铂的、成本低的和资源丰富的催化剂<sup>[6-12]</sup>。其中, 杂原子掺杂碳催化剂有较高的氧还原反应 (Oxygen Reduction Reaction, ORR) 催化活性和耐甲醇渗透性, 被认为是可替代铂基催化剂的燃料电池新催化剂<sup>[13-19]</sup>。本文综述了近年来杂原子掺杂碳材料 ORR 催化剂的研究进展。

## 1 杂原子掺杂碳催化理论

杂原子掺杂碳催化剂是一类  $sp^2$  杂化碳基催化材料。 $sp^2$  杂化碳材料表面有可自由迁移的  $\pi$  电子<sup>[16]</sup>。因此, 对电子参与的电化学反应 (如 ORR),  $sp^2$  杂化碳材料有可能成为潜在的催化剂<sup>[17]</sup>。然而, 无掺杂的电中性的碳材料并无电催化活性<sup>[21]</sup>, 只能通过掺杂改变  $sp^2$  杂化的碳原子的电中性, 掺杂元素无论富电子原子 (如 N) 或贫电子原子 (如 B) 均可构成具有电催化活性的 ORR 催化剂。掺杂原子如 O、N、B、P、S、I 等<sup>[18-34]</sup>被引入碳结构后, 因其与碳原子键长、价电子和原子尺寸不同, 相邻碳原子附近位点出现缺陷, 电荷分布不均匀, 碳材料的电中性受破坏, 更有利于构筑氧分子吸附和还原的活性中心<sup>[18-19]</sup>。此外, Mn、Co、Fe 等金属盐也常作为催化剂或氧化剂用于制备  $sp^2$  杂化碳材料 (如石墨烯、碳纳米管等), 在后续处理时这些金属元素难

以从碳材料中彻底清除。即便  $sp^2$  杂化碳材料中残余金属仅为仪器可检测下限, 其在碱性介质氧还原仍不可忽视<sup>[20]</sup>。

## 2 杂原子掺杂碳催化剂

### 2.1 氧掺杂

氧杂原子一般以含氧官能团形式掺杂于碳材料的石墨结构中。对碳材料而言, 这种掺杂方式几乎难以避免, 且永久伴随。即便充分地还原, 含氧官能团也难以完全除去。在异相反应及纳米金属颗粒负载的过程, 氧杂原子提供了反应活性位点, 故通常可在石墨化的碳晶格中引入含氧官能团, 以增强碳材料的反应性。通过石墨氧化、超声剥离及化学还原的方法制备出还原氧化石墨烯, 如图 1<sup>[35]</sup>。得益于高比表面和含氧官能团, 还原氧化石墨烯在碱性溶液中有明显的氧还原催化活性。此外, 碳石墨晶格中的氧杂原子可以在一定条件下被 N、B 等元素原位取代, 为其他元素掺杂提供了一条简便快捷的路径。

### 2.2 氮掺杂

氮原子与碳原子有相似的原子半径 (氮原子半径略小于碳), 但其电负性更大, 已广泛用于元素掺杂。氮掺杂有两种方式: 原位掺杂或称为前掺杂, 即在形成石墨结构时同步掺入氮原子; 后者后掺杂, 即对碳材料经氧化、热处理、取代等后处理

收稿日期: 2014-05-14, 修订日期: 2014-06-16 \* 通讯作者, Tel: (86-23)65105161, E-mail: zdwei@cqu.edu.cn

国家自然科学基金项目 (No. 20936008, No. 21176271, No. 21276291) 及中央高校科研业务费重大研究项目 (No. CD-JZR12228802) 资助

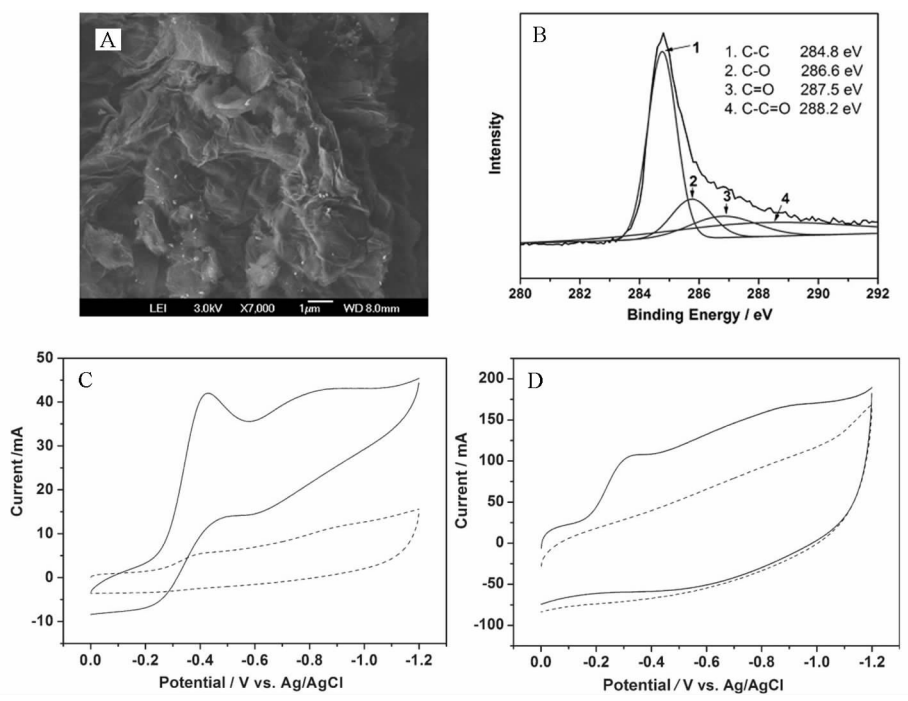


图 1 还原氧化石墨烯的扫描电镜照片(A)和 C1s XPS 谱图(B);玻碳电极(C)和还原氧化石墨烯修饰电极(D)在氧气(实线)和氩气(虚线)饱和的 0.1 mol·L<sup>-1</sup> KOH 溶液的循环伏安曲线<sup>[35]</sup>

Fig. 1 SEM image (A) and XPS C1s spectra (B) of rGSFs; Cyclic voltammograms obtained at bare GC (C) and rGSF/GC (D) electrodes in 0.10 mol·L<sup>-1</sup> KOH solution saturated with Ar (dashed lines) or O<sub>2</sub> (solid lines) Scan rate: 100 mV·s<sup>-1</sup><sup>[35]</sup>

掺入氮原子.氮掺入石墨结构碳纳米材料(如碳纳米管、石墨烯、微孔石墨层以及无定形碳等)引起基体材料原子结构变形、增加碳的 *n*-型导电性,改变原子结构和电子结构,形成有 *sp*<sup>2</sup> 杂化碳结构的离域共轭体系,致使碳材料宏观性质(如电子、机械、结构、反应性和电催化性能)显著改变<sup>[10,28,34,36-41]</sup>.通过化学气相沉积法(CVD)制得氮掺杂碳纳米管阵列(VA-NCNTs),在碱性溶液中与 Pt/C 一样显示优异 ORR 电催化活性和稳定性,如图 2 所示<sup>[10]</sup>.在 VA-NCNTs 的氧还原按 4 电子过程进行,且可抗 CO 中毒.N 原子(3.04)较 C 原子(2.55)有更大的电负性,可使其相邻 C 原子产生正电荷密度,更利于 O<sub>2</sub> 的表面吸附及 O—O 键断裂.

作者课题组采用改性的 CVD 法,以二茂铁为碳源和催化剂、三聚氰胺和尿素为氮源制得两种不同的竹状结构氮掺杂碳纳米管(NCNT)<sup>[42]</sup>,如图 3 所示.三聚氰胺(M)氮源较尿素(U)氮源制得的 NCNT 具有更高的氮含量、更多的缺陷,说明氮前驱物对掺氮量以及催化剂结构有很大的影响.

除碳纳米管掺氮外,其他碳材料也可掺杂氮杂原子并表现出优异的氧还原电催化活性. Mal-

donado 和 Stevenson<sup>[43]</sup>合成了 N 掺杂碳纳米纤维(N-CNF),可更容易吸附 O<sub>2</sub>,并促进过氧化氢的分解. pH < 10 时,N-CNF 电极还原 O<sub>2</sub> 为 2 电子反应,速率控制步骤系过氧化氢吸附. pH > 10 时,O<sub>2</sub> 吸附过程受过氧化氢的质子化速率控制.该催化剂在碱性介质中可促进过氧化氢质子化,从而提高 ORR 电催化活性. Chen 等<sup>[44]</sup>制备了高比表面积、高氮含量掺杂碳纳米笼催化剂,该催化剂氧还原电催化为 4 电子过程.在碱性介质中 ORR 的电催化活性和稳定性均优于商业化 Pt/C. Jin 等<sup>[45]</sup>将 N 掺杂于碳干凝胶中,在酸性条件下有一定的 ORR 电催化活性和良好的稳定性. Ma 等<sup>[46]</sup>报道了在碱性介质中,与 Pt/C 催化剂电催化活性相当的 N 掺杂中空碳纳米粒子(N-HCNPs),且 N-HCNPs 有更好的稳定性,以及耐甲醇渗透性和抗 CO 中毒性. Yu 等<sup>[47]</sup>制备了 3D 多孔结构 N 掺杂多孔石墨烯(NHG)作为 ORR 和肼氧化的多功能催化剂. 3D 多孔结构可减少石墨烯片与片的密堆积,更利于反应物 / 电解质在片层之间的传递. 包信和等<sup>[48]</sup>报道了大批量高质量氮掺石墨烯的方法,如图 4 所示.采用溶剂热反应将四氯化碳和氮化锂直接反

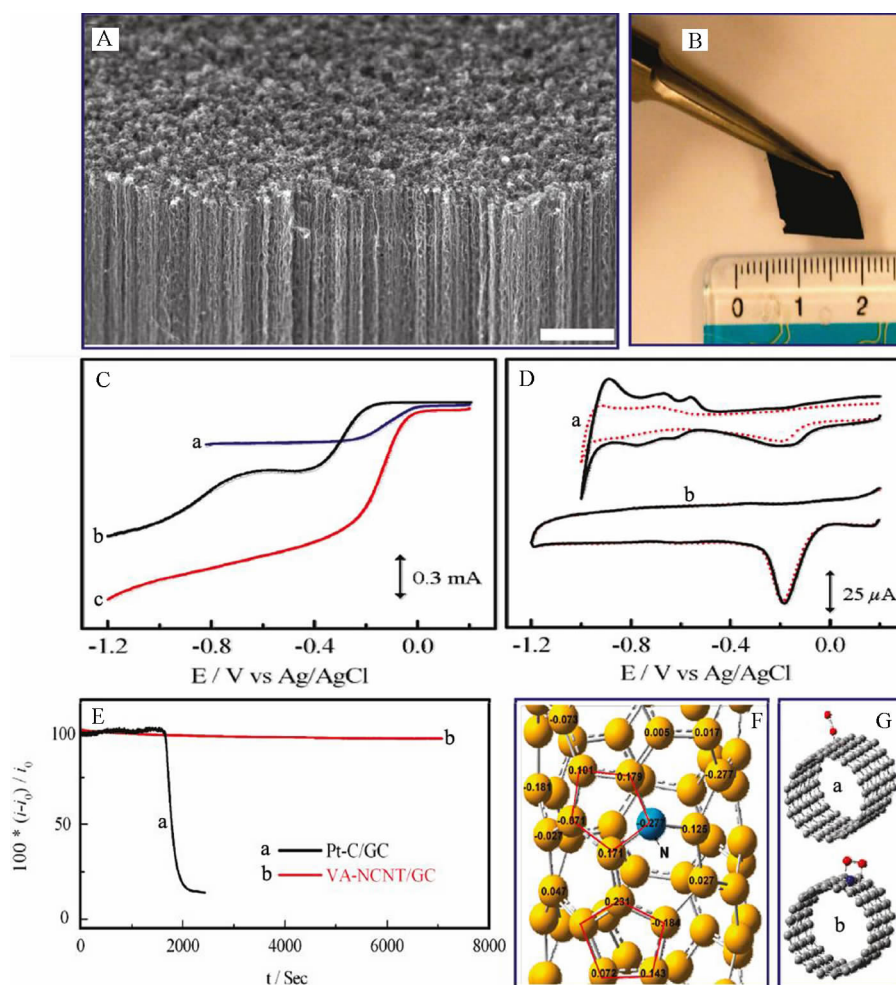


图 2 A. VA-NCNTs 的 SEM 照片; B. VA-NCNTs 膜的数码相机照片; C. Pt-C(a)、VA-CCNT(b) 和 VA-NCNT(c) 旋转圆盘电极在空气饱和的  $0.1 \text{ mol} \cdot \text{L}^{-1}$  KOH 溶液中对 ORR 的伏安曲线; D. 100 000 r 动电位扫描前(实线)和后(虚线)的 Pt-C (a) 和 VA-NCNT(b) 电极的 ORR 循环伏安曲线, 扫描速率为  $100 \text{ mV} \cdot \text{s}^{-1}$ ; E. Pt-C(a) 和 VANCNT(b) 电极 CO 中毒效应的计时电流响应曲线.  $55 \text{ mL} \cdot \text{min}^{-1}$  CO 气体(先通入  $550 \text{ mL} \cdot \text{min}^{-1}$   $\text{O}_2$  气流, 而后通入含  $\sim 9\%$  CO(V/V) 的混合气体, 通气时间约为 1700 s); F. NCNTs 的电荷密度分布; G. CCNTs(a) 和 NCNTs(b) 材料氧分子可能吸附模式的示意图<sup>[10]</sup>

Fig. 2 A. SEM image of the as-synthesized VA-NCNTs; B. Digital photograph of the VANCNT array; C. RRDE voltammograms in air saturated  $0.1 \text{ mol} \cdot \text{L}^{-1}$  KOH solution at the Pt-C/GC (a), VA-CCNT/GC (b), and VA-NCNT (c) electrodes; D. CVs for the ORR at the Pt-C/GC (a) and VA-NCNT/GC (b) electrodes before (solid lines) and after (dotted lines) a continuous potentiodynamic swept for  $\sim 100\,000$  cycles in an air saturated  $0.1 \text{ mol} \cdot \text{L}^{-1}$  KOH solution; E. CO-poison effect on the  $i-t$  chronoamperometric response for the Pt-C/GC (a) and VA-NCNT/GC (b) electrodes; F. Calculated charge density distribution for the NCNTs; G. Schematic representations of possible adsorption modes of an oxygen molecule at the CCNTs (a) and NCNTs (b)<sup>[10]</sup>

应生成氮掺杂的石墨烯, 实现了克量级制备氮掺杂石墨烯。陈军等<sup>[49]</sup>在氧化石墨烯表面, 以 Fe 催化三聚氰胺热解, 实现 Fe-N 同时掺杂石墨烯和碳纳米管的同步合成路线, 如图 5 所示。该复合催化剂中纳米管分散均匀、管径均一, 其特殊的 3D 结构有利于提高传质和电催化活性。

包信和等<sup>[50]</sup>将金属铁纳米粒子包裹在氮掺杂

纳米管中制得豆荚状催化剂, 如图 6、7 所示。该催化体系中, 铁金属颗粒不与酸性介质、氧和硫等污染物直接接触, 也不妨碍活化氧分子电催化氧还原反应。DFT 计算表明, 铁粒子的电荷转移降低了碳纳米管表面的局部功函从而形成 ORR 电催化活性中心。

掺氮碳材料中, 氮有 5 种键合结构(如图 8),



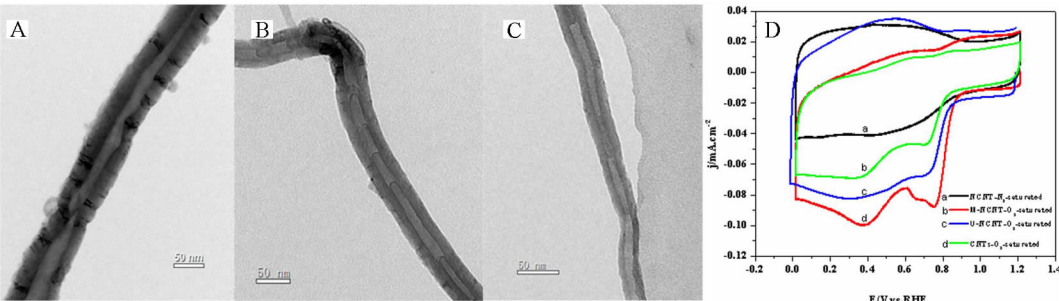


图 3 碳纳米管(A)、三聚氰胺-氮掺杂碳纳米管(B)和尿素-碳纳米管(C)的透射电镜照片,各种碳纳米管在氧气饱和的 0.1 mol·L<sup>-1</sup> KOH 溶液中的循环伏安曲线(D)<sup>[42]</sup>

Fig. 3 TEM images of CNTs (A), M-NCNT (B) and U-NCNT (C); Cyclic voltammograms on M-NCNT/CG, U-NCNT and CNTs/CG rotating disk electrodes in 0.1 mol·L<sup>-1</sup> KOH solution saturated with N<sub>2</sub> or O<sub>2</sub> (D)<sup>[42]</sup>

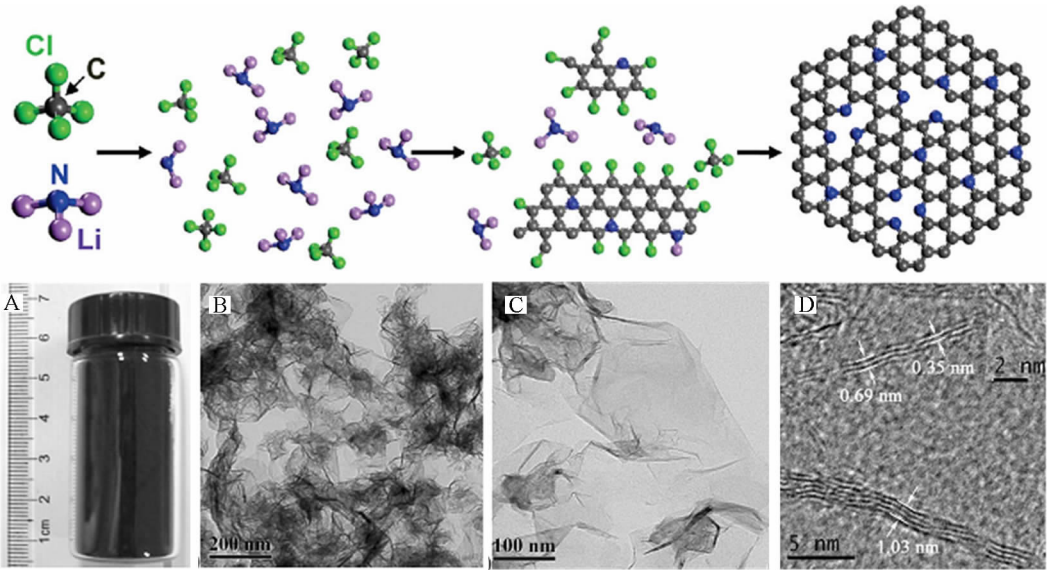


图 4 溶剂热法氮掺杂石墨烯制备示意图:A. 40 mL 反应釜,1.2 g NG;B-C. 不同倍率 TEM 照片;D. 高分辨电镜照片<sup>[48]</sup>

Fig. 4 Scheme of a proposed mechanism for solvothermal synthesis of N-doped graphene via the reaction of CCl<sub>4</sub> and Li<sub>3</sub>N. A. Vial containing NG-1 (1.2 g) obtained with a 40 mL autoclave per batch in the laboratory; B-C. TEM images of NG-2 at differentmagnifications; D. HRTEM images of NG-1 showing the cross sections of single (inserted image) to four-layer graphene<sup>[48]</sup>

分别为石墨氮、吡啶氮、吡嗪氮、氨基氮以及氧化氮。哪一种掺氮碳材料氧还原电催化活性最好,目前尚有争议。吡啶氮掺杂的石墨烯,其 ORR 的过程系 2 电子还原过程,据此认为吡啶氮不是有效的 ORR 催化中心<sup>[51]</sup>。与此相反,还有发现,酸性条件下催化剂还原活性随吡啶氮含量增加而升高<sup>[52]</sup>;在碱性介质,其电催化活性随吡嗪氮含量增加而升高<sup>[53]</sup>。故氮掺杂碳材料的活性中心须考虑如下要点:首先,氮键合结构不同时,其催化剂的导电性是否处于同一水平;再者,催化剂中 sp<sup>2</sup> 杂化 C 含

量、石墨化程度是否一致。通常,石墨氮形成的温度较高,更有利于碳材料石墨化,也影响着材料的导电性和 sp<sup>2</sup> 杂化 C 结构。因此,“高石墨氮含量-高 ORR 活性”可能与碳基材料的导电性有关。此外,大部分氮掺杂碳材料通常仅适用于碱性条件的 ORR 反应而在酸性介质则中难以适用。

采用乙腈<sup>[54]</sup>和乙二胺<sup>[55]</sup>制备的 N 掺杂碳纳米管(N-CNTs)较纯碳纳米管(CNTs)在 0.5 mol·L<sup>-1</sup> H<sub>2</sub>SO<sub>4</sub> 呈现出更高的 ORR 活性。N-CNTs 掺入的氮元素可以改变 CNTs 在酸性条件的 ORR 反应稳定

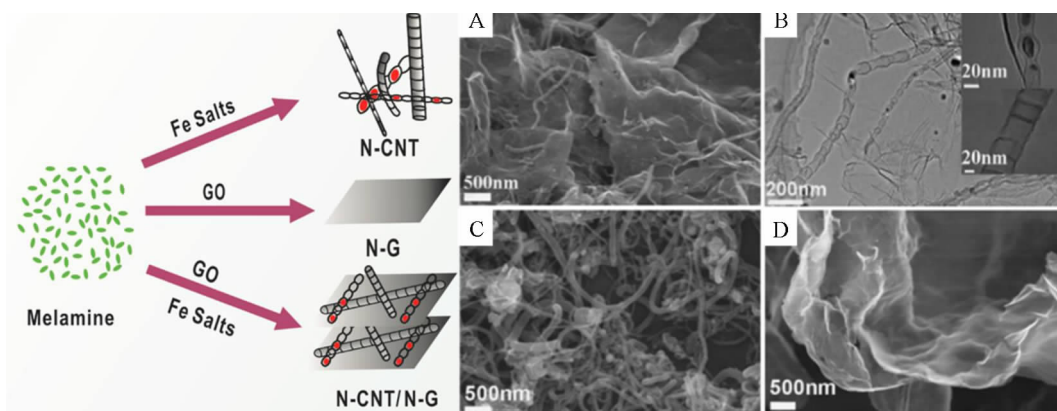


图 5 N-CNT、N-G 及 N-CNT/N-G 复合物制备示意图. A-B. Fe-N 掺杂碳纳米管 / 石墨烯复合物的 SEM 照片和 TEM 照片 (B 中内插图是为复合物中单个碳纳米管的高分辨 TEM 照片); C. 碳纳米管的 SEM 照片; D. 石墨烯的 SEM 照片<sup>[49]</sup>

Fig. 5 Schematic illustration of the formation of the N-CNT, N-G and N-CNT/N-G composite

A-B. SEM and TEM images of the N-CNT/N-G composite (inset of B: High resolution TEM images of the individual CNTs in the composite); C. SEM image of the N-CNT composite; D. SEM image of the N-G composite<sup>[49]</sup>

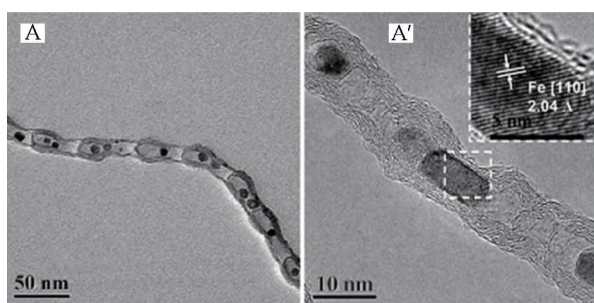


图 6 Pod-Fe 催化剂的透射电镜照片(A)与高分辨透射电镜照片(A')<sup>[50]</sup>

Fig. 6 TEM image (A) and HRTEM image (A') of Pod-Fe with the inset showing the [110] crystal plane of the Fe particle<sup>[50]</sup>

性.  $\text{NH}_3$  后处理的氮掺杂介孔碳材料在  $0.05 \text{ mol} \cdot \text{L}^{-1} \text{H}_2\text{SO}_4$  中同样具有一定的 ORR 活性<sup>[36]</sup>. 然而, 大量研究表明, 非金属催化剂的氧还原活性在酸性介质较商业化 Pt/C 依然很弱. 在碱性电解质中, 非金属催化剂的氧还原半波电位与商业化 Pt/C 催化剂之差在 25 mV 以内, 而酸性介质其差则大于 200 mV. 酸性介质体系平面结构的吡啶氮和吡咯氮氧还原电催化更为重要, 是氧还原的电催化中心<sup>[51-52, 54-59]</sup>. 季氨氮则由于键角的褶皱结构降低了催化活性点的导电性, 其并非 ORR 催化活性点. 如何在高度石墨化的条件下选择性的合成平面氮(吡啶氮和吡咯氮)以抑制季氨氮的形成则是获得高活性 ORR 催化剂的关键.

如图 9 所示, 作者课题组研究“NG 分子结构

-NG 电导率 -ORR 催化活性”的关联, 利用层状材料(LM)的层间限域效应, 通过调制 LM 层间距, 获得平面氮掺杂达 90% 以上的 NG 材料<sup>[59]</sup>. 其 ORR 的半波电位仅较 Pt/C 催化剂的差 60 mV, 获得的 NG 材料 ORR 电催化活性则为传统材料电催化活性的 54 倍, 该催化剂正极的质子交换膜燃料电池的输出功率可达  $320 \text{ mW} \cdot \text{cm}^{-2}$  (图 10).

### 2.3 其他元素掺杂

掺杂元素如 B、P、S 等电子结构和原子尺寸均与 C 相似, 这些原子掺杂碳材料燃料电池阴极催化剂时也表现出较好的电催化活性. B 掺杂缺电子的碳纳米管中, B 的 2pz 空轨道与 C 的  $\pi$  体系结合使  $\pi$  电子活化,  $\text{O}_2$  分子极易在 B 正电荷位点还原<sup>[60]</sup>. 研究表明, B 掺杂碳纳米管在碱性环境中有良好的电催化稳定性、耐甲醇渗透性和抗 CO 中毒性<sup>[18]</sup>. P 掺杂石墨片层在碱性介质中也具有较好的 ORR 电催化活性<sup>[10]</sup>, 其 ORR 电催化活性与碳材料比表面积以及 P 的掺杂量有极大的关系. 作者课题组通过六氟磷酸盐离子液体辅助法合成了 P 掺杂的石墨烯纳米片(P-TRG), 如图 11 所示<sup>[61]</sup>. 该法获得的 P-TRG 比表面大 ( $496.67 \text{ m}^2 \cdot \text{g}^{-1}$ ), P 原子掺杂水平高 (1.16%), 在碱性环境下较 Pt/C 有更为优异的氧还原电催化活性. 以共价键形式掺入石墨化结构中的 P 原子在热处理过程部分氧化为磷氧官能团. 掺杂 P 的石墨烯产生了许多波纹与开放的边缘位点, 较纯石墨烯其 P-TRG 的孔径和孔体积均扩大, 其 BET 比表面积从初始的  $195.72 \text{ m}^2 \cdot \text{g}^{-1}$

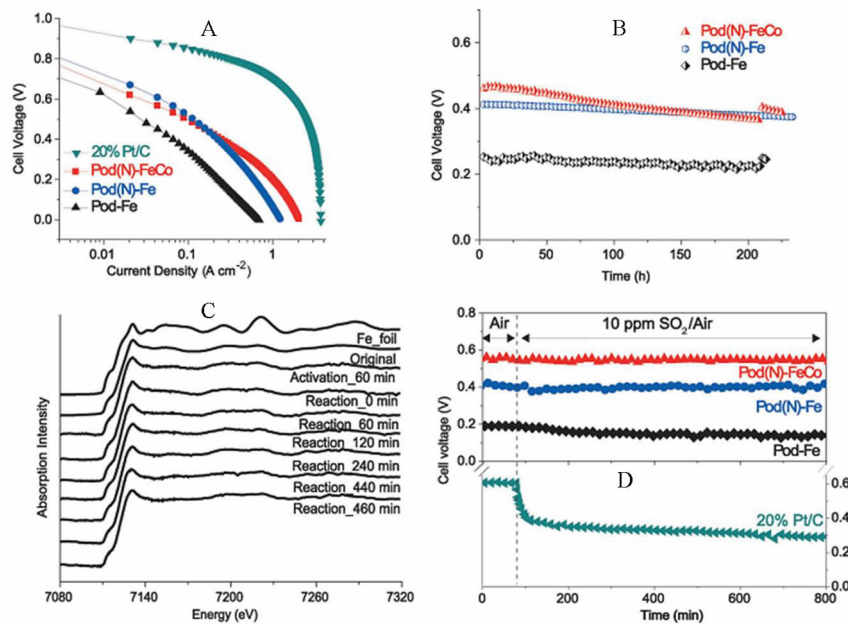


图 7 A. Pod-Fe, Pod(N)-Fe, Pod(N)-FeCo 氢氧燃料电池极化曲线;B. 氢氧燃料电池稳定曲线;C. 燃料电池 Pod-Fe 催化剂 XANES 在线测试曲线;D. 10 mL·m<sup>-3</sup> SO<sub>2</sub> 条件下电池稳定性曲线<sup>[50]</sup>

Fig. 7 A. Cell voltage-current density and B. cell voltage-time curves for a H<sub>2</sub>-O<sub>2</sub> single fuel cell; C. *In situ* Fe K-edge XANES of Pod-Fe cathode under PEMFC operation conditions; D. Durability test in the presence of 10 mL·m<sup>-3</sup> SO<sub>2</sub> in air with Pod-Fe, Pod(N)-Fe, Pod(N)-FeCo, and commercial 20% Pt/C (JM) cathodes<sup>[50]</sup>

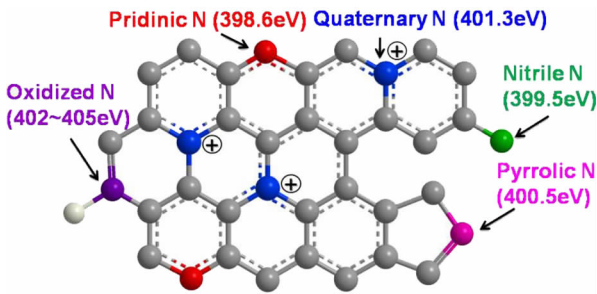


图 8 石墨结构氮掺入位置以及相应的结合能数据<sup>[59]</sup>

Fig. 8 Typical structures and binding energies given for quaternary, pyrrolic, pyridinic and pyridinic-oxide nitrogen groups<sup>[59]</sup>

增至 496.67 m<sup>2</sup>·g<sup>-1</sup>. S 掺杂石墨烯阴极非金属催化剂有两种典型形式:硫化物官能团(—C—S—C—)和硫氧化物官能团(—C—SO<sub>x</sub>—C,  $x = 2 \sim 4$ , 如硫酸盐或磺酸盐)<sup>[26]</sup>. 在较高温度退火过程中,硫氧化物官能团能够转化成硫化物官能团. 其中,C—S 键可能构成重要的催化活性位点, 高温退火提高 S 掺杂催化剂的电催化活性,如图 12 所示. 此外,碳材料经 VII 族如 F<sup>[62]</sup>、I<sup>[17]</sup>掺杂也表现出较好的 ORR 电催化活性和稳定性.

2.4 多元掺杂

通过多元素掺杂引入第二种“活性”元素,调

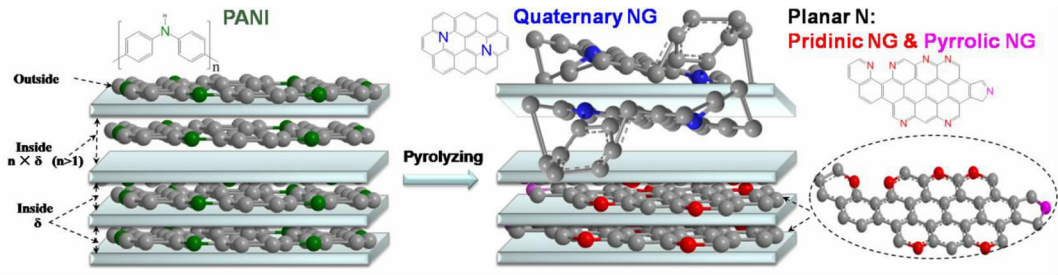


图 9 层状材料调控选择性合成平面氮掺杂石墨烯示意图<sup>[59]</sup>

Fig. 9 Schematic representation showing the selectiviies inside and outside of MMT during NG synthesis<sup>[59]</sup>



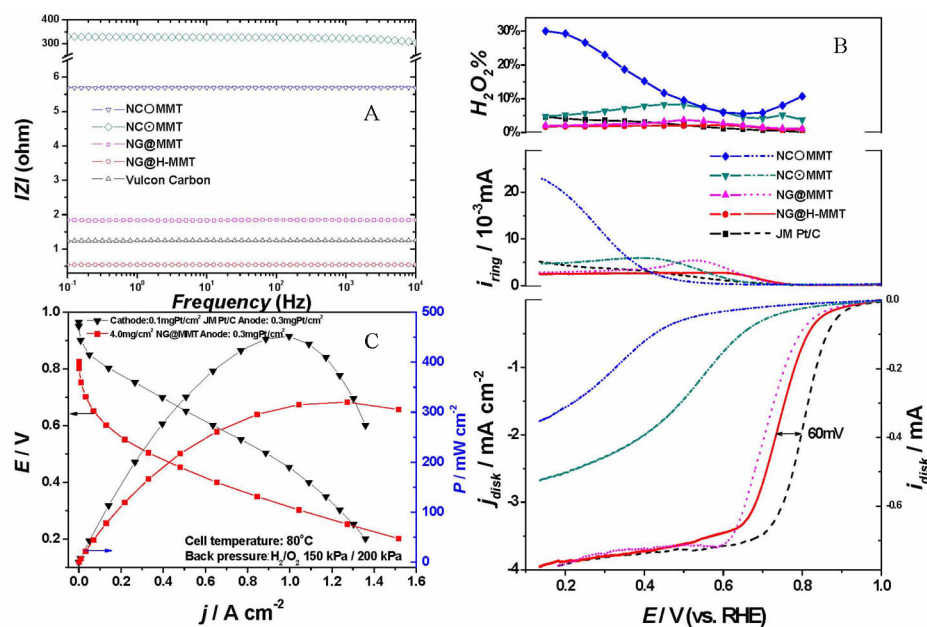


图 10 层状材料调控合成平面氮掺杂石墨烯的导电性测试(A), 旋转圆盘电极测试(B)和单电池的性能曲线(C)<sup>[59]</sup>

Fig. 10 A. Bode spectra obtained through the application of a sine wave with an amplitude of 5.0 mV from 10 mHz to 10 kHz for different catalysts; B. Steady-state plots of ORR polarization (bottom), ring current (middle), and  $\text{H}_2\text{O}_2$  yield (top) for different catalysts in  $\text{O}_2$ -saturated  $0.1 \text{ mol} \cdot \text{L}^{-1} \text{ HClO}_4$  solution; C. Polarization curves and corresponding power densities of membrane electrode assemblies fabricated with the NG@MMT cathode catalyst<sup>[59]</sup>

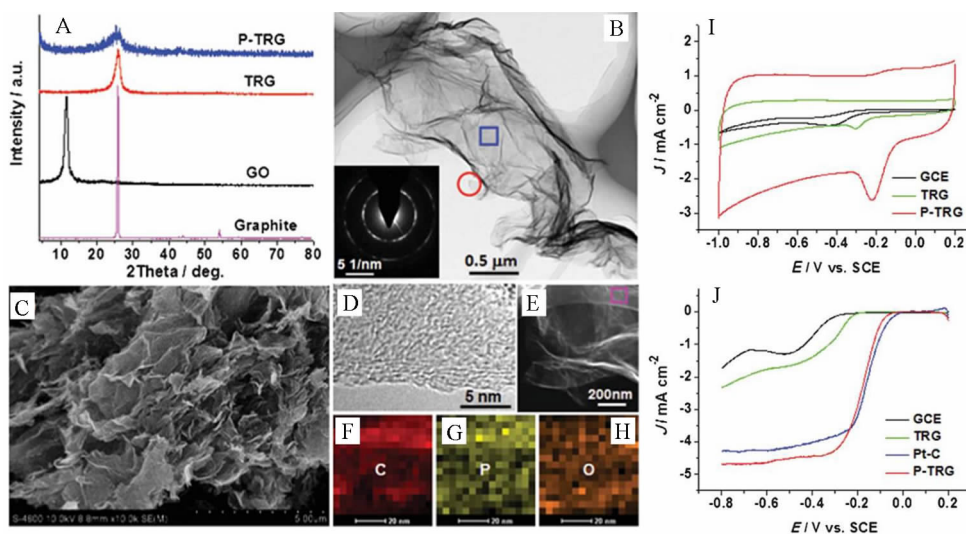


图 11 A. P-TRG, TRG 和 GO 的 XRD 谱图; B. P-TRG 的扫描电镜照片 (内插图 B 中方形区域的电子衍射图谱); C. P-TRG 的透射电镜照片; D. B 中圆形区域的高分辨透射电镜; E. B 中方形区域的扫描透射电镜照片; F-H. B 中方形区域的元素能谱图片; I. 各样品在  $\text{O}_2$  饱和的  $0.1 \text{ mol} \cdot \text{L}^{-1} \text{ KOH}$  溶液中循环伏安曲线; J. 各样品在  $\text{O}_2$  饱和的  $0.1 \text{ mol} \cdot \text{L}^{-1} \text{ KOH}$  溶液中氧还原极化曲线<sup>[61]</sup>

Fig. 11 A. XRD patterns of the as-prepared P-TRG, TRG, and GO as well as the original graphite powder; B. Typical SEM image of the P-TRG sample (inset shows the SAED pattern of the rectangle area); C. Typical TEM images of the P-TRG sample; D. HRTEM image of the circled area in panel B; E. STEM image of the corresponding elemental mappings of the rectangle area in B; F-H. The corresponding elemental mappings of the rectangle area in B; I. CV curves of the ORR at various electrodes at a scan rate of  $100 \text{ mV} \cdot \text{s}^{-1}$  in  $\text{O}_2$ -saturated  $0.1 \text{ mol} \cdot \text{L}^{-1} \text{ KOH}$  solution; J. LSV curves of the ORR at various electrodes in  $\text{O}_2$ -saturated  $0.1 \text{ mol} \cdot \text{L}^{-1} \text{ KOH}$  solution at a scan rate of  $5 \text{ mV} \cdot \text{s}^{-1}$  and rotation rate of  $1600 \text{ r} \cdot \text{min}^{-1}$ <sup>[61]</sup>

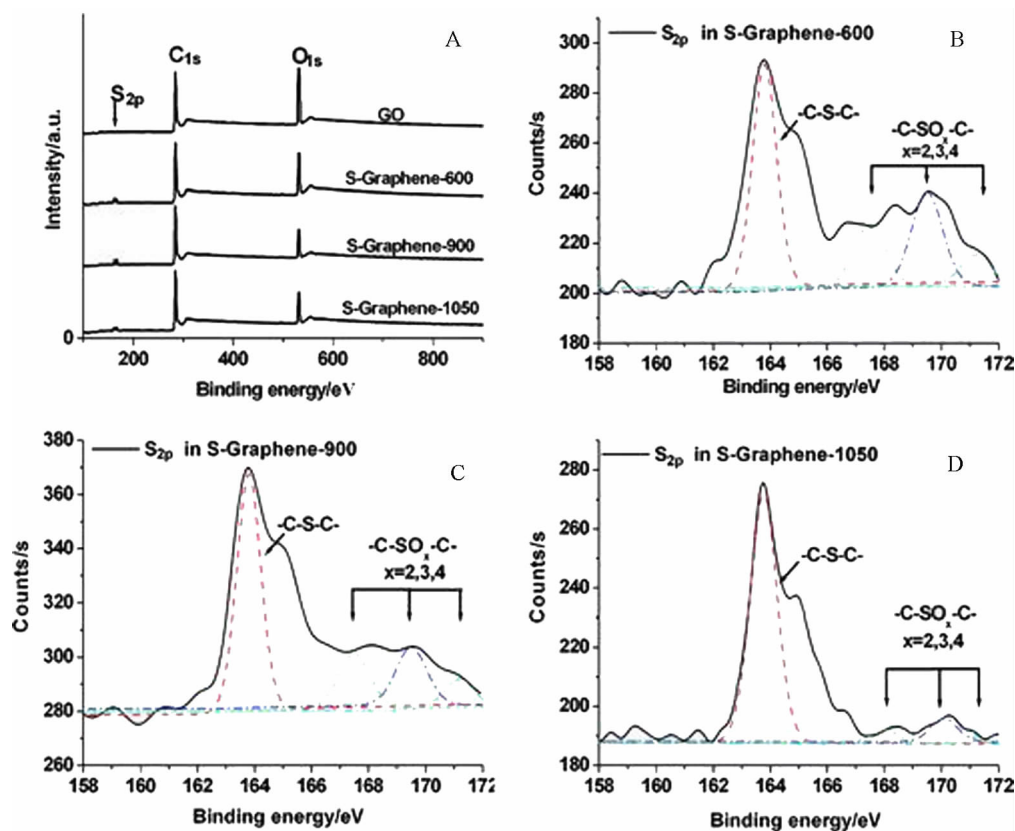


图 12 A. GO、S-graphene-600、S-graphene-900 和 S-graphene-1050 的 XPS 谱图; B-D. S-graphene-600、S-graphene-900 和 S-graphene-1050 的高分辨  $S_{2p}$  谱图<sup>[26]</sup>

Fig. 12 A. XPS spectra of GO, S-graphene-600, S-graphene-900, and S-graphene-1050; B-D. High-resolution  $S_{2p}$  spectra of S-graphene-600, S-graphene-900, and S-graphene-1050<sup>[26]</sup>

控掺杂原子的数量、比例,改善催化协同效应,以增强催化剂的 ORR 活性<sup>[63]</sup>. B、N 二元掺杂单层石墨烯中由于 B、N、C 之间形成多种杂化键,使其具有独特的电子性能<sup>[64-65]</sup>. 将 B 掺杂到 N 掺杂碳材料中形成了新 B-N-C 活性位点增强了 ORR 电催化活性<sup>[66]</sup>. Choi 等<sup>[67]</sup>和 Subramanian 等<sup>[68]</sup>报道 S 和 N 掺杂碳二元催化剂在酸性介质中的 ORR 电催化活性比一元 N 掺杂或 S 掺杂碳催化剂的更高. Choi 等<sup>[69]</sup>将 P 掺入 N 掺杂碳中制得 P、N 二元催化剂. P 的掺入改变了碳的形貌,增加了基材的比表面积,产生更多的 ORR 活性位点,从而使得该催化剂的电催化活性更高. P 掺入量增加,其 ORR 电催化活性先增后降,10%(by mass)P 掺入量催化剂的电催化活性最优,如图 13. 掺入 P 原子后增加了碳材料的缺陷位点,杂原子掺入量过多时碳材料的  $sp^2$  结构坍塌,无法提供高效的电子通道,阻碍了三相界面( $O_2$ 、质子、电子)的形成. S 和 N 二元掺杂微孔石墨烯催化剂<sup>[70]</sup>、B 和 N 共掺杂垂直排列

的碳纳米管<sup>[71]</sup>有第二活性位点的引入,增强了 ORR 电催化活性,而二元掺杂催化剂的 ORR 活性的改善不是简单叠加,而是多种原子相互耦合的协同效应.

Hu 等<sup>[21]</sup>利用直接气相沉积法合成 B、N 二元催化剂,在高温热处理过程生成硼氮结合物(BN),掺杂元素的结合降低催化剂的电催化活性. 如图 14 所示,B 掺入量的增加,BN 结合的 N 掺杂碳纳米管较 B/N 分开存在的 N 掺杂碳纳米管的起始电位和峰电流均低(图 9). 采用硼酸(或氨)溶解剥离氧化石墨烯的方法制得 B- 和 N- 掺杂石墨烯(B,N-graphene),若高度掺杂,石墨烯含大量绝缘的 BN 簇,ORR 过程的电子转移将十分困难<sup>[72]</sup>.

### 3 结 论

替代 Pt 类高效低成本的非金属催化剂是燃料电池商业化的关键. 探究非金属催化剂的活性与原子组成、电子构型、表面形貌的构效关系,构筑功能性的复合非金属催化剂,以期提高非金属催



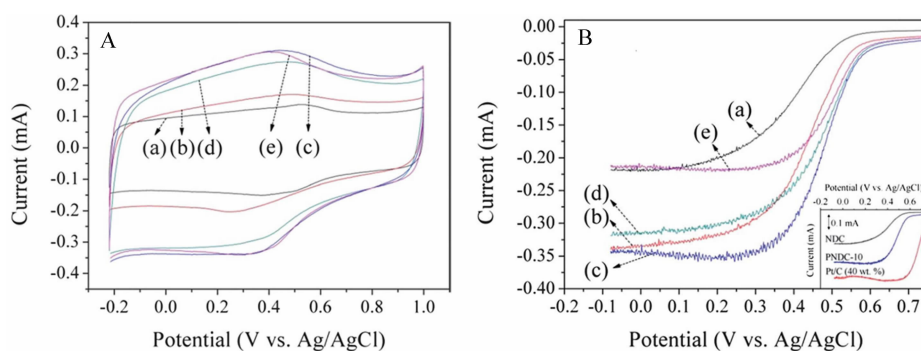


图 13 NDC (a)、PNDC-5 (b)、PNDC-10 (c)、PNDC-15 (d)和 PNDC-20 (e)在  $1 \text{ mol} \cdot \text{L}^{-1} \text{HClO}_4$  中的 CV 曲线(A)和在  $\text{O}_2$  饱和的  $1 \text{ mol} \cdot \text{L}^{-1} \text{HClO}_4$  溶液中的 ORR 电催化活性曲线(B)<sup>[69]</sup>

Fig. 13 CV (A) and ORR activities (B) in  $\text{O}_2$  saturated  $1 \text{ mol} \cdot \text{L}^{-1} \text{HClO}_4$  results NDC (a), PNDC-5 (b), PNDC-10 (c), PNDC-15 (d), and PNDC-20 (e) in deaerated  $1 \text{ mol} \cdot \text{L}^{-1} \text{HClO}_4$ <sup>[69]</sup>

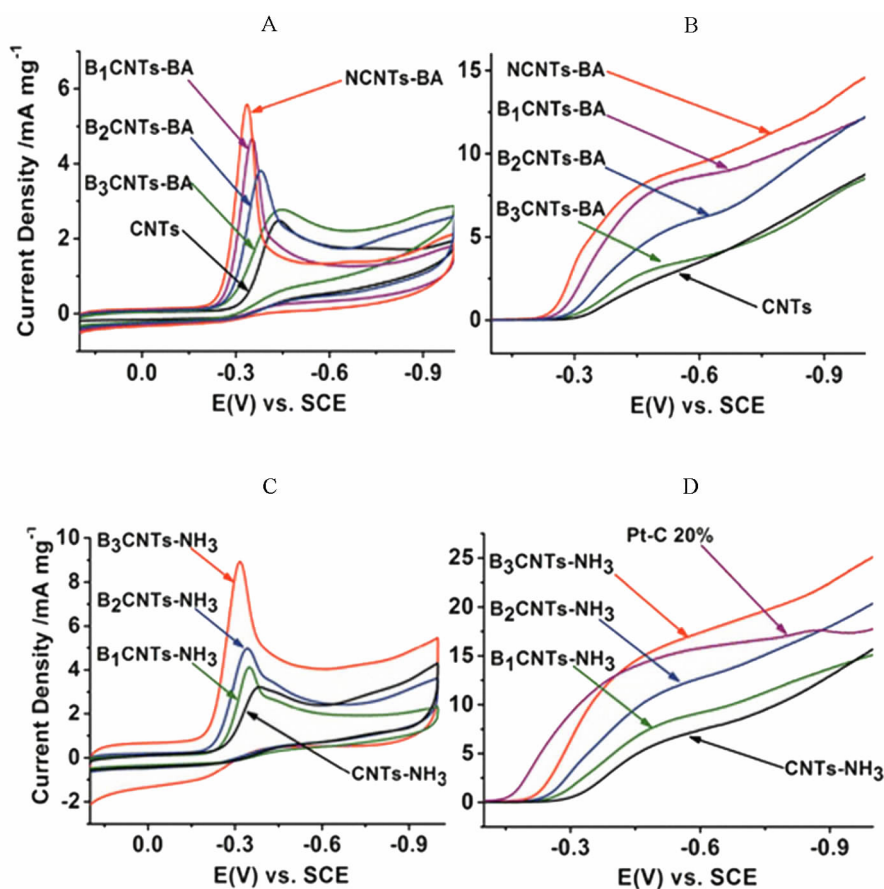


图 14 在  $\text{O}_2$  饱和的  $1 \text{ mol} \cdot \text{L}^{-1} \text{NaOH}$  溶液中 BCNTs-BA(结合态的 B 和 N)和 BCNTs-NH<sub>3</sub>(分开存在的 B 和 N)催化剂的 CV 曲线(A,C,扫速:  $50 \text{ mV} \cdot \text{s}^{-1}$ )和 RDE 曲线(B,D,扫速:  $10 \text{ mV} \cdot \text{s}^{-1}$ ,转速:  $2500 \text{ r} \cdot \text{min}^{-1}$ )<sup>[21]</sup>

Fig. 14 Electrocatalytic capabilities of the BCNTs-NH<sub>3</sub> catalysts for ORR in  $\text{O}_2$ -saturated  $1 \text{ mol} \cdot \text{L}^{-1} \text{NaOH}$  electrolyte. A, C. CV at a scan rate of  $50 \text{ mV} \cdot \text{s}^{-1}$ . B, D. RDE at a scan rate of  $10 \text{ mV} \cdot \text{s}^{-1}$  and rotation speed of  $2500 \text{ r} \cdot \text{min}^{-1}$ <sup>[21]</sup>

化剂的耐蚀性和稳定性, 研发大功率低温燃料电池的非金属催化剂必将是今后研发工作的重要方向.

### 参考文献(References):

- [1] Chen S G, Wei Z D, Guo L, et al. Enhanced dispersion and durability of Pt nanoparticles on a thiolated CNT support

- [J]. Chemical Communications, 2011, 47: 10984-10986.
- [2] Chen S G, Wei Z D, Qi X Q, et al. Nanostructured polyaniline-decorated Pt/C@PANI core@shell catalyst with enhanced durability and activity[J]. Journal of the American Chemical Society, 2012, 134(32): 13252-13255.
- [3] Chen S. G, Wei Z D, Li H, et al. High Pt utilization PEM-FC electrode obtained by alternative ion-exchange/electrodeposition[J]. Chemical Communications, 2010, 46: 8782-8784.
- [4] Luo J(罗瑾), Yang L F(杨乐夫), Chen B H(陈秉辉), et al. Ternary alloy electrocatalysts for oxygen reduction reaction[J]. Journal of Electrochemistry(电化学), 2012, 18(6): 496-507.
- [5] Lv H F(吕海峰), Cheng N C(程年才), Mu S C(木士春), et al. Electrocatalytic properties of Pd modified Pt/C catalysts for proton exchange membrane fuel cell[J]. Acta Chimica Sinica(化学学报), 2009, 67(14): 1680-1684.
- [6] Jasinski R. A new fuel cell cathode catalyst[J]. Nature, 1964, 201: 1212-1213.
- [7] Lee J, Aida T. "Bucky gels" for tailoring electroactive materials and devices: The composites of carbon materials with ionic liquids[J]. Chemical Communications, 2011, 47: 6757-6762.
- [8] Maruyama J, Abe I. Structure control of a carbon-based noble-metal-free fuel cell cathode catalyst leading to high power output[J]. Chemical Communications, 2007, 27: 2879-2881.
- [9] Liang Y Y, Li Y G, Wang H L, et al. Co<sub>3</sub>O<sub>4</sub> nanocrystals on graphene as a synergistic catalyst for oxygen reduction reaction[J]. Nature Materials, 2011, 10: 780-786.
- [10] Gong K P, Du F, Xia Z H, et al. Nitrogen-doped carbon nanotube arrays with high electrocatalytic activity for oxygen[J]. Science, 2009, 323(5915): 760-764.
- [11] Zhang J, Sasaki K, Sutter E, et al. Stabilization of platinum oxygen-reduction electrocatalysts using gold clusters[J]. Science, 2007, 315(5809): 220-224.
- [12] Sun Y Q, Li C, Xu Y X, et al. Chemically converted graphene as substrate for immobilizing and enhancing the activity of a polymeric catalyst[J]. Chemical Communications, 2010, 46: 4740-4742.
- [13] Wang G J, Cheng F, Yu Y, et al. SC-IrO<sub>2</sub>NR-carbon hybrid: A catalyst with high electrochemical stability for oxygen reduction[J]. SCIENCE CHINA Chemistry, 2013, 56(1): 131-136.
- [14] Dai X F(戴先逢), Zhen M F(郑明富), Xu P(徐攀), et al. Electrochemical behavior of pyridine-doped carbon-supported Co-Phthalocyanine (Py-CoPc/C) for oxygen reduction reaction and its application to fuel cell[J]. Acta Physico-Chimica Sinica (物理化学学报), 2013, 29(8): 1753-1761.
- [15] Serov A, Kwak C. Review of non-platinum anode catalysts for DMFC and PEMFC application[J]. Applied Catalysis B-Environmental, 2009, 90(3/4): 313-320.
- [16] Su D S, Zhang J, Frank B, et al. Metal-free heterogeneous catalysis for sustainable chemistry [J]. ChemSusChem, 2010, 3(2): 169-180.
- [17] Winther-Jensen B, Winther-Jensen O, Forsyth M, et al. High rates of oxygen reduction over a vapor phase-polymerized PEDOT electrode[J]. Science, 2008, 321(5889): 671-674.
- [18] Yang L J, Jiang S J, Zhao Y, et al. Boron-doped carbon nanotubes as metal-free electrocatalysts for the oxygen reduction reaction[J]. Angewandte Chemie-International Edition, 2011, 50(31): 7132-7135.
- [19] Liu Z W, Peng F, Wang H J, et al. Phosphorus-doped graphite layers with high electrocatalytic activity for the O<sub>2</sub> reduction in an alkaline medium [J]. Angewandte Chemie-International Edition, 2011, 50(14): 3257-3261.
- [20] Wang L, Ambrosi A, Pumera M. "Metal-free" catalytic oxygen reduction reaction on heteroatom-doped graphene is caused by trace metal impurities [J]. Angewandte Chemie-International Edition, 2013, 52(51): 13818-13821.
- [21] Zhao Y, Yang L J, Hu Z, et al. Can boron and nitrogen Co-doping improve oxygen reduction reaction activity of carbon nanotubes? [J]. Journal of the American Chemical Society, 2013, 135(4): 1201-1204.
- [22] Okamoto Y. First-principles molecular dynamics simulation of O<sub>2</sub> reduction on nitrogen-doped carbon [J]. Applied Surface Science, 2009, 256(1): 335-341.
- [23] Qu L, Liu Y, Baek J, et al. Nitrogen-doped graphene as efficient metal-free electrocatalyst for oxygen reduction in fuel cells [J]. ACS Nano, 2010, 4(3): 1321-1326.
- [24] Yang S, Feng X L, Wang X C, et al. Graphene-based carbon nitride nanosheets as efficient metal-free electrocatalysts for oxygen reduction reactions [J]. Angewandte Chemie-International Edition, 2011, 50(23): 5339-5343.
- [25] Sheng Z H, Gao H L, Bao W J, et al. Synthesis of boron doped graphene for oxygen reduction reaction in fuel cells [J]. Journal of Materials Chemistry, 2012, 22(2): 390-395.
- [26] Yang Z, Yao Z, Li G F, et al. Sulfur-doped graphene as an efficient metal-free cathode catalyst for oxygen reduction [J]. ACS Nano, 2012, 6(1): 205-211.
- [27] Yao Z, Nie H G, Yang Z, et al. Catalyst-free synthesis of iodine-doped graphene via a facile thermal annealing process and its use for electrocatalytic oxygen reduction in an alkaline medium [J]. Chemical Communications,

- 2012, 48(7):1027-1029.
- [28] Liu R L, Wu D Q, Feng X L, et al. Nitrogen-doped ordered mesoporous graphitic arrays with high electrocatalytic activity for oxygen reduction[J]. *Angewandte Chemie-International Edition*, 2010, 49(14): 2565-2569.
- [29] Shao Y Y, Zhang S, Engelhard M H, et al. Nitrogen-doped graphene and its electrochemical applications[J]. *Journal of Materials Chemistry*, 2010, 20(35): 7491-7496.
- [30] Yu D S, Zhang Q, Dai L M, et al. Highly efficient metal-free growth of nitrogen-doped single-walled carbon nanotubes on plasma-etched substrates for oxygen reduction[J]. *Journal of the American Chemical Society*, 2010, 132(43): 15127-15129.
- [31] Wang S Y, Yu D S, Dai L M, et al. Polyelectrolyte functionalized carbon nanotubes as efficient metal-free electrocatalysts for oxygen reduction[J]. *Journal of the American Chemical Society*, 2011, 133(14): 5182-5185.
- [32] Yu D S, Nagelli E, Du F, et al. Metal-free carbon nanomaterials become more active than metal catalysts and last longer[J]. *Journal of Physical Chemistry Letters*, 2010, 1(14): 2165-2173.
- [33] Wang X, Lee J, Zhu Q, et al. Ammonia-treated ordered mesoporous carbons as catalytic materials for oxygen reduction reaction[J]. *Chemistry of Materials*, 2010, 22(7): 2178-2180.
- [34] Zhang J, Liu X, Blume R, et al. Surface-modified carbon nanotubes catalyze oxidative dehydrogenation of *n*-butane[J]. *Science*, 2008, 322(5898): 73-77.
- [35] Longhua T, Ying W, et al. Preparation, structure, and electrochemical properties of reduced graphene sheet films[J]. *Advanced Functional Materials*, 2009, 19(17): 2782-2789.
- [36] Okotrub A V, Bulusheva L G, Kudashov A G, et al. Orientation ordering of N<sub>2</sub> molecules in vertically aligned CN<sub>x</sub> nanotubes [J]. *Applied Physics A-Materials Science & Processing*, 2009, 94(3): 437-443.
- [37] Biddinger E J, Deak D V, Ozkan U S. Nitrogen-containing carbon N as oxygen-reduction catalysts[J]. *Topics in Catalysis*, 2009, 52(11): 1566-1574.
- [38] Sun C L, Wang H W, Hayashi M, et al. Atomic-scale deformation in N-doped carbon nanotubes[J]. *Journal of the American Chemical Society*, 2006, 128(26): 8368-8369.
- [39] Terrones M, Ajayan P M, Terrones H, et al. N-doping and coalescence of carbon nanotubes: Synthesis and electronic properties[J]. *Applied Physics A-Materials Science & Processing*, 2002, 74(3): 355-361.
- [40] Panchakarla L S, Govindaraj A, Rao C N R. Nitrogen-and boron-doped double-walled carbon nanotubes [J]. *ACS Nano*, 2007, 1(5): 494-500.
- [41] Wong W Y, Daud W R W, Mohamad A B, et al. Recent progress in nitrogen-doped carbon and its composites as electrocatalysts for fuel cell applications[J]. *International Journal of Hydrogen Energy*, 2013, 38(22): 9370-9386.
- [42] Xiong K, Wei Z D, et al. Nitrogen-doped carbon nanotubes as catalysts for oxygen reduction reaction [J]. *Journal of Power Sources* 2012, 215: 216-220
- [43] Maldonado S, Stevenson K J. Influence of nitrogen doping on oxygen reduction electrocatalysis at carbon nanofiber electrodes[J]. *Journal of Physical Chemistry B*, 2005, 109(10): 4707-4716.
- [44] Chen S, Wang X Z, Hu Z, et al. Nitrogen-doped carbon nanocages as efficient metal-free electrocatalysts for oxygen reduction reaction[J]. *Advanced Materials*, 2012, 24(41): 5593-5597.
- [45] Jin H, Zhang H M, Zhong H X, et al. Nitrogen-doped carbon xerogel: A novel carbon-based electrocatalyst for oxygen reduction reaction in proton exchange membrane (PEM) fuel cells[J]. *Energy & Environmental Science*, 2011, 4(9): 3389-3394.
- [46] Ma G X, Jia R R, Zhao J H, et al. Nitrogen-doped hollow carbon nanoparticles with excellent oxygen reduction performances and their electrocatalytic kinetics[J]. *Journal of Physical Chemistry C*, 2011, 115(50): 25148-25154.
- [47] Yu D S, Wei L, Chen Y, et al. Nitrogen doped holey graphene as an efficient metal-free multifunctional electrochemical catalyst for hydrazine oxidation and oxygen reduction[J]. *Nanoscale*, 2013, 5(8): 3457-3464.
- [48] Deng D H, Pan X L, Yu L, et al. Toward N-doped graphene via solvothermal synthesis[J]. *Chemistry of Materials*, 2011, 23(5): 1188-1193.
- [49] Zhang S M, Zhang H Y, Chen S. L, et al. Fe-N doped carbon nanotube/graphene composite: Facile synthesis and superior electrocatalytic activity[J]. *Journal of Materials Chemistry A*, 2013, 1(10): 3302-3308.
- [50] Deng D H, Yu L, Chen X Q, et al. Iron encapsulated within pod-like carbon nanotubes for oxygen reduction reaction [J]. *Angewandte Chemie-International Edition*, 2012, 52(1): 371-375.
- [51] Luo Z Q, Lim S H, Lin J Y, et al. Pyridinic N doped graphene: Synthesis, electronic structure, and electrocatalytic property[J]. *Journal of Materials Chemistry*, 2011, 21(22): 8038-8044.
- [52] Rao C V, Cabrera C R, Ishikawa Y. Search of the active site in nitrogen-doped carbon nanotube electrodes for the oxygen reduction reaction[J]. *Journal of Physical Chemistry Letters*, 2010, 1(18): 2622-2627.



- [53] Unni S M, Devulapally S, et al. Graphene enriched with pyrrolic coordination of the doped nitrogen as an efficient metal-free electrocatalyst for oxygen reduction[J]. *Journal of Materials Chemistry*, 2012, 22(44): 23506-23513.
- [54] Kundu S, Nagaia T C, Muhler M, et al. Electrocatalytic activity and stability of nitrogen-containing carbon nanotubes in the oxygen reduction reaction [J]. *Journal of Physical Chemistry C*, 2009, 113(32): 14302-14310.
- [55] Dorjgotov A, Ok J, Jeon Y K, et al. Activity and active sites of nitrogen-doped carbon nanotubes for oxygen reduction reaction[J]. *Journal of Applied Electrochemistry*, 2013, 43(4):387-397.
- [56] Sidik R A, Anderson A B, Subramanian N P, et al. O<sub>2</sub> reduction on graphite and nitrogen-doped graphite: Experiment and theory[J]. *Journal of Physical Chemistry B*, 2006, 110(4): 1787-1793.
- [57] Liang Y Y, Li Y G, Wang H L, et al. Co<sub>3</sub>O<sub>4</sub> nanocrystals on graphene as a synergistic catalyst for oxygen reduction reaction[J]. *Nature Materials*, 2011, 10(10): 780-786.
- [58] Wang S Y, Zhang L P, Xia Z H, et al. BNC graphene as efficient metal-free electrocatalyst for the oxygen reduction[J]. *Angewandte Chemie-International Edition*, 51(17): 4209-4212.
- [59] Ding W, Wei Z D, Chen S G, et al. Space-confinement-induced synthesis of pyridinic- and pyrrolic-nitrogen-doped graphene for the catalysis of oxygen reduction[J]. *Angewandte Chemie-International Edition*, 2013, 52(45): 11755-11759.
- [60] Yang L J, Jiang S J, Zhao Y, et al. Boron-doped carbon nanotubes as metal-free electro catalysts for the oxygen reduction reaction [J]. *Angewandte Chemie-International Edition*, 2011, 50(31): 7132-7135.
- [61] Li R, Wei Z D, Gou X L, et al. Phosphorus-doped grapheme nanosheets as efficient metal-free oxygen reduction electrocatalysts[J]. *RSC Advances*, 2013, 3(25): 9978-9984.
- [62] Sun X J, Xu W L, Xing W, et al. Fluorine-doped carbon blacks: Highly efficient metal-free electrocatalysts for oxygen reduction reaction[J]. *ACS Catalysis*, 2013, 3(8): 1726-1729.
- [63] Choi C H, Park S H, Woo S I. Binary and ternary doping of nitrogen, boron, and phosphorus into carbon for enhancing electrochemical oxygen reduction activity [J]. *ACS Nano*, 2012, 6(8): 7084-7091.
- [64] Ci L J, Song L, Ajayan P M, et al. Atomic layers of hybridized boron nitride and graphene domains[J]. *Nature Materials*, 2010, 9(5): 430-435.
- [65] Ci L J, Song L, Yakobson B I, et al. Large scale growth and characterization of atomic hexagonal boron nitride layers[J]. *Nano Letters*, 2010, 10(8): 3209-3215.
- [66] Ozaki J I, Kimura N, Oya A, et al. Preparation and oxygen reduction activity of BN-doped carbons[J]. *Carbon*, 2007, 45(9): 1847-1853.
- [67] Choi C H, Park S H, Woo S I. Heteroatom doped carbons prepared by the pyrolysis of bio-derived amino acids as highly active catalysts for oxygen electro-reduction reactions[J]. *Green Chemistry*, 2011, 13(2): 406-412.
- [68] Subramanian N P, Nallathambi V, Popov B N, et al. Nitrogen-modified carbon-based catalysts for oxygen reduction reaction in polymer electrolyte membrane fuel cells [J]. *Journal of Power Sources*, 2009, 188(1): 38-44.
- [69] Choi C H, Park S H, Woo S I. Phosphorus-nitrogen dual doped carbon as an effective catalyst for oxygen reduction reaction in acidic media: Effects of the amount of P-doping on the physical and electrochemical properties of carbon[J]. *Journal of Materials Chemistry*, 2012, 22(24): 12107-12115.
- [70] Liang J, Jiao Y, Qiao S Z, et al. Sulfur and nitrogen dual-doped mesoporous graphene electrocatalyst for oxygen reduction with synergistically enhanced performance [J]. *Angewandte Chemie-International Edition*, 2012, 51(46): 11496-11500.
- [71] Wang S Y, Roy A, Dai L M, et al. Vertically aligned BCN nanotubes as efficient metal-free electrocatalysts for the oxygen reduction reaction: A synergetic effect by Co-doping with boron and nitrogen [J]. *Angewandte Chemie-International Edition*, 2011, 50(49): 11756-11760.
- [72] Wang S Y, Zhang L P, Dai L M, et al. BCN graphene as efficient metal-free electrocatalyst for the oxygen reduction reaction [J]. *Angewandte Chemie-International Edition*, 2012, 51(17): 4209-4212.

## Recent Progress in Heteroatoms Doped Carbon Materials as a Catalyst for Oxygen Reduction Reaction

DING Wei<sup>1</sup>, ZHANG Xue<sup>1,2</sup>, LI Li<sup>1</sup>, WEI Zi-dong<sup>1\*</sup>

(1. *School of Chemistry and Chemical Engineering, Chongqing University, Chongqing 400044, China;*

2. *College of Chemistry and Chemical Engineering, Xiamen University, Xiamen 361005, Fujian, China*)

**Abstract:** Developing catalytic materials for oxygen reduction reactions (ORR) with high performance and low cost has been one of the major challenges for large-scale applications of fuel cells. In this review, we summarize the recent progress in the heteroatoms doped carbon materials as a catalyst for the catalysis of ORR, with an emphasis on the universal origin of their catalytic mechanisms. The future prospects of the metal-free catalyst were to find precisely controlled doping methods, to explore the role of heteroatoms in the catalysis, and to generate more active catalysts with suitable nanostructure.

**Key words:** fuel cell; oxygen reduction reaction; electrocatalysis; heteroatom-doped carbon materials